ISBN: 978-3-95450-223-3 ISSN: 2673-7000 doi:10.18429/JACoW-NAPAC2019-TUZBA2

# ELECTRON ION COLLIDER MACHINE DETECTOR INTERFACE*

B. Parker†, E.C. Aschenauer, A. Kiselev, C. Montag, R. B. Palmer, V. Ptitsyn, F.J. Willeke, H. Witte,
Brookhaven National Laboratory, Upton, Long Island, NY, USA
M. Diefenthaler, Y. Furletova, T.J. Michalski, V.S. Morozov, D. Romanov, A. Seryi, R. Yoshida,
Thomas Jefferson National Accelerator Facility, Newport News, VA, USA
C. Hyde, Old Dominion University, Norfolk, VA, USA
M.K. Sullivan, SLAC National Accelerator Laboratory, Menlo Park, CA, USA

*Abstract*

Here we review the major physics requirements, accelerator challenges and some magnet design issues for the Machine Detector Interface (MDI) of an Electron Ion Collider (EIC) Interaction Region (IR). In order to fully exploit the rich physics potential of an EIC, an IR MDI team must balance a complex interplay that arises when combining hadron and electron collider accelerators in an optimized IR. The work described in this paper results from ongoing close collaboration between many people at BNL, JLab and other institutes to realize an EIC as the next, highest priority, future nuclear physics project.

## EIC MDI CONSIDERATIONS

HERA at DESY, which collided unpolarized protons with a self-polarized electron beam, was the only ep-collider built so far. HERA opened new areas of investigation and gave new questions to explore; subsequent studies led to establishing an EIC Physics White Paper as a guide for future EIC physics requirements [1-4]. Some EIC detector and accelerator requirements taken from the White Paper are outlined in Table 1, where we also compare the existing state of the art LHC and RHIC physics parameters to the EIC design requirements [5-7].

HERA experience, especially from the HERA-II upgrade, shows that hadronic beam gas and synchrotron radiation (direct and backscatter) backgrounds can significantly impact the physics data taking; such backgrounds are do not a dominate background source at other hadron colliders.

Further compounding EIC measurement difficulty is the need to detect particles traveling very close to the circulating beams due to the kinematics of the physics process. Also, the natural optimization path for providing the highest possible EIC luminosity leads to colliding many bunches at high frequency (i.e. short bunch spacing) and at much larger total crossing angles than considered for the LHC. Reaching a high EIC luminosity, obtainable with a Crab Crossing scheme, is essential do a wide range of precision physics and is especially critical for studies involving polarization dependent observables.

While the rapid beam separation enabled via a large crossing angle allows colliding bunches at high frequency, the short bunch spacing is a significant factor for choosing appropriate EIC detector technologies. Finally, we will see that some aspects of the EIC physics program favor using a crossing angle instead of depending upon beam separation dipoles as was done at HERA.

In the idealized EIC detector shown in Fig.1, we see events where the scattered electron, #1, and particles associated with the struck parton, #3, are detected in the central solenoid region; however, sometimes particles associated

Table 1: Some ways that EIC challenges are different from other colliders. Here we compare EIC to the LHC and RHIC. The differences impact both EIC detector acceptance and the choice of possible detector technologies that can be used.

| EIC | LHC / RHIC |
|---|---|
| **Collide different beam species: ep and eA** | **Collide the same species: pp, pA and AA** |
| → Hadron beam backgrounds, i.e. beam gas events | → Hadron backgrounds, i.e. beam gas and high pile up |
| → Synchrotron radiation related backgrounds | |
| **Asymmetric Beam Energies** | **Symmetric Beam Energies** |
| → Boosted kinematics → high activity at high $\|\eta\|$ | → Not boosted → Most activity at mid rapidity |
| **High Repetition Rate** | **Moderate Repetition Rate** |
| → 2 – 9 ns spacing between bunches | → 25 ns spacing between bunches |
| **Large Crossing Angle** | **No crossing Angle…Yet** |
| → Crab Crossing: 25 – 50 mrad | → Any future LHC angle would be very much smaller |
| **Wide Range of Center of Mass Energies** | **Limited Range of Center of Mass Energies** |
| EIC → Factor 7 | LHC → Factor 2 |
| | RHIC → Factor 26 in AA and 8 in pp |
| **EIC Both Beams Are Polarized** | **LHC No Beam Polarization / RHIC Polarized pp** |
| → Polarized Stat. Uncertainty: ~ $1/(P_1P_2(\int L\,dt)^{1/2})$ | → LHC Unpolarized Stat. Uncertainty: ~$1/(\int L\,dt)^{1/2}$ |

* Work supported by U.S. Department of Energy, Office of Nuclear Physics under contracts: DE-SC0012704 and DE-AC05-06OR23177.
† email address : parker@bnl.gov

ISBN: 978-3-95450-223-3 ISSN: 2673-7000 doi:10.18429/JACoW-NAPAC2019-TUZBA2

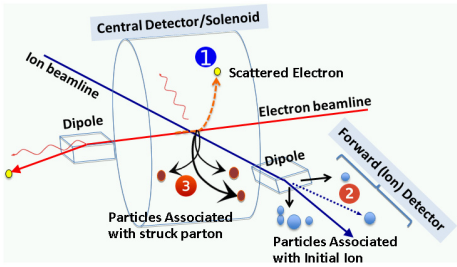


Figure 1: An idealized EIC physics detector.

with the initial ion, #2, exit close to the circulating hadron beam in the forward direction. Following HERA convention, the side where the circulating hadron beam exits is denoted as the forward side.

For some low $Q^2$ physics, it is critical to detect when a scattered electron exits close to the circulating electron beam on the rear side (i.e. side where the circulating electron beam exits). For each beam there are dipoles located outside the detector that only deflect one or the other beam. Near the central detector the beams are still very close together; this closeness foreshadows a major IR magnet design headache, the need to shield circulating beams from external magnetic fields from neighboring beamline magnets. The much lower-energy electron beam is quite sensitive to stray fields and challenging to protect.

In what follows we note that while the two IR designs are functionally equivalent, both BNL (eRHIC) and JLab (JLEIC) have made specific IR design choices that differ slightly in detail due to local considerations and the choice of what center of mass energy to optimize for; both designs provide options to cover all White Paper physics goals and both share common MDI challenges.

For example, Fig. 2 shows the eRHIC IR design implementation (JLEIC IR layout is shown later in Fig. 4). Fig. 2 is intended to highlight the available aperture for each magnet with respect to the multiple particle types that the magnet must let pass. For MDI considerations a central region of ±4.5 m from the interaction point (IP) is set aside just for the detector with no machine elements. To achieve the require hadron magnet field strengths the ±20 m region of the IP uses superconducting magnets. Note that the magnet layouts on the forward (right) and rear (left) side of Fig. 2 are quite different. The forward side hadron magnet apertures are significantly larger than on the rear side due to physics acceptance requirements. In turn the rear side electron magnet apertures are larger than for the forwards side electron magnets in order to cleanly pass the synchrotron radiation fan generated by the upstream forward side electron IR quadrupoles.

Both the eRHIC and JLEIC IR designs have crossing angles with Crab Crossing for beam separation instead of using separation dipoles (as used for HERA and planned for the LHeC) [8-10]. A representative example of an EIC detector using a crossing angle beam separation scheme with Crab Crossing is the JLEIC detector shown in Fig. 3.

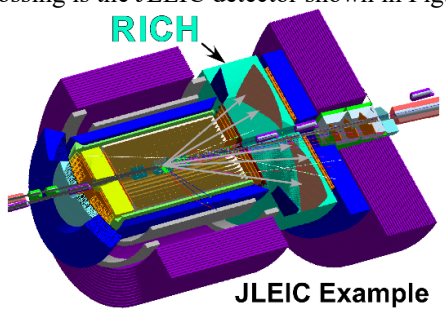


Figure 3: EIC detector showing projected lines in RICH.

One clear motivation for choosing a crossing angle geometry for an EIC is to avoid generating strong synchrotron radiation upstream of the detector that could hit material either inside the detector or close by downstream to cause background. While this is a notable consideration, it is EIC physics requirements that ultimately drive using a crossing angle despite the attendant complication of having to operate Crab Cavities to effectively reestablish head-on bunch collisions [11].

Putting separation dipoles deep inside an EIC detector blocks too much critical physics acceptance thanks to kinematics of the physics process. We also studied integrating a large-radius, low-field dipole coil with the main solenoid but this has other drawbacks. First off, the dipole field leads to considerable non-azimuthally-symmetric acceptance variations at small forward scattering angles. A second consideration is that EIC semi-inclusive deep inelastic scattering requires very clean particle identification (PID). The only practical way we find to meet demanding EIC PID requirements is to use a gaseous Ring Imaging Cherenkov Detector (RICH) which has well known magnetic field limitations.

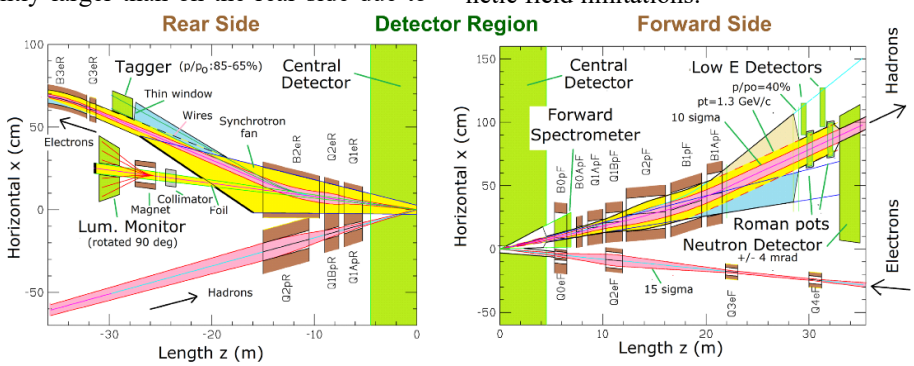


Figure 2: EIC IR layout schematic. Here the eRHIC version of the EIC IR layout is shown; the JLEIC IR (shown in Fig. 4) is functionally similar but makes different choices for the crossing angle (eRHIC 25 mrad, JLEIC 50 mrad) and electron polarimeter location, i.e. choices driven by two different base accelerator designs.

ISBN: 978-3-95450-223-3 ISSN: 2673-7000 doi:10.18429/JACoW-NAPAC2019-TUZBA2

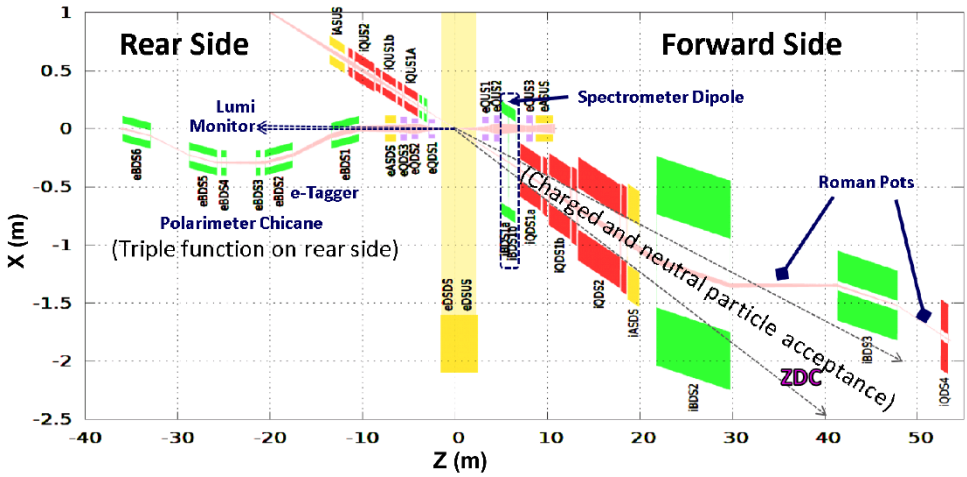


Figure 4: JLEIC IR layout schematic with 50 mrad crossing angle and nearby electron polarimeter chicane.

In order not to smear RICH rings due to Cerenkov light, charged particles should follow straight lines inside the RICH volume. Ideally there should be no overlapping magnetic field, or at least the magnetic field lines should be "projective in the RICH" (i.e. aligned with particle trajectories), for negligible magnetic deflection and performance degradation. For the LHeC there is no gaseous RICH detector (i.e. there is no PID which works at several 100 GeV particle energy) so the LHeC IR layout can use a large-radius detector integrated separation dipole.

The JLEIC IR layout shown in Fig. 4 and the Fig. 2 eRHIC layout are functionally very similar; they both have very large aperture, forward side, hadron magnets. The forward hadron apertures in both IR designs reflect the need for multiple beam separation stages. After the electron and hadron beams are in independent beam pipes (thanks to the crossing angle), the circulating hadron beam must be separated from both neutrons associated with physics events and from other forward charged particles having different magnetic rigidity than the hadron beam. These forward going charged particles are at angles too small to be detected in the central solenoid. The kinematics for one important class of such charged particles, forward protons, is shown on Fig. 5.

The neutrons come out in a cone spread around the IP hadron direction and travel to a dedicated detector, the Zero Degree Calorimeter (ZDC) along with small angle photons. One important motivation for the ZDC is illustrated by Fig. 6 with a comparison of the expected differential cross sections for eAu events. The events of special interest undergo a coherent process where the residual Au nucleus remains intact. These diffractive events are easily swamped by an incoherent background where the Au nucleus breaks up. Fortunately, the incoherent background can be suppressed by detecting these break-up neutrons and photons at the ZDC. The relationship between momentum and angle for break-up events at different center of mass (CM) values, as shown in Fig. 7, informs what angular acceptance is needed for the ZDC.

Efficiently detecting the break-up neutrons requires forward hadron magnets with at least ±4 mrad angular acceptance. This implies that the hadron IR quadrupole apertures and coil fields get progressively larger and quite hard to accommodate with increasing distance from the IP; the combination of large apertures and large coil fields makes shielding the electrons from coil leakage fields a significant magnet design challenge. Both IR layouts use very large aperture hadron dipoles to deflect charged particles away from the neutron cone going to the ZDC.

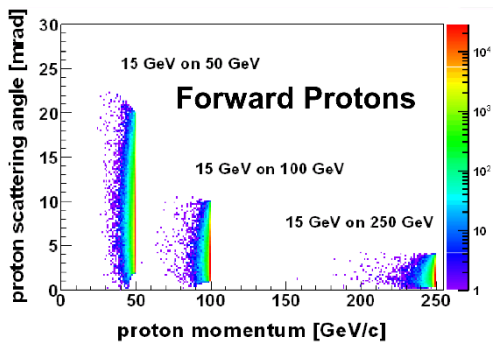


Figure 5: Relationship of forward proton momentum and angle for 15 GeV electrons against the three different indicated proton beam energies of 250, 100 and 50 GeV.

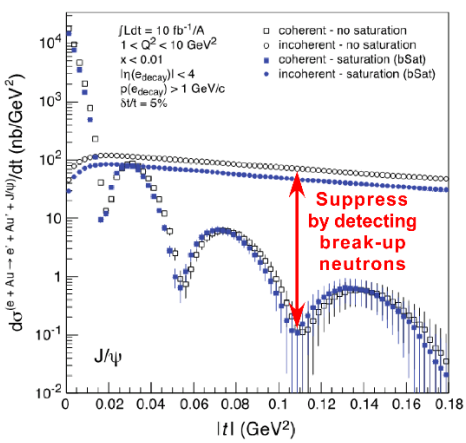


Figure 6: An eA diffractive physics plot that illustrates an EIC design requirement. We use a forward neutron detection veto to suppress the incoherent background where the struck nucleus (here Au) does not remain intact.

ISBN: 978-3-95450-223-3 ISSN: 2673-7000 doi:10.18429/JACoW-NAPAC2019-TUZBA2



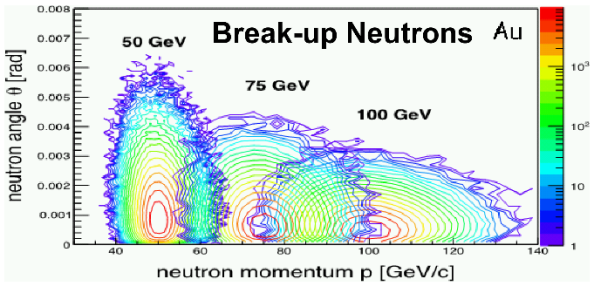


Figure 7: Relationship of neutron momentum and angle for eAu break-up events at three different CM energies.

Both designs use a spectrometer dipole close to the central detector to measure intermediate angle forward particles that would not pass through the later IR quadrupole apertures. As stated earlier, the charged particles that do get through are deflected by large aperture dipoles located after these quadrupoles. It is at this point that the JLEIC and eRHIC IR optimizations diverge [12-16]. The IR layouts and their corresponding forward magnet apertures reflect a different balance between what is detected inside the spectrometer dipole versus later detection in dedicated Roman Pot detectors, i.e. moveable silicon detectors that can go very close to the circulating hadron beam.

Both designs look to keep all IR magnet coil peak fields at a level where well understood NbTi superconducting technology can be used. The eRHIC IR design passes ±5 mrad forward protons to the Roman Pots (accepting the 250 GeV proton beam cluster in Fig. 5) while measuring the rest in the spectrometer dipole. The JLEIC IR design has ±10 mrad forward acceptance to the Roman Pots (accepting the 100 and 250 GeV proton beam clusters in Fig. 5) and therefore specifies larger aperture superconducting magnets that then take advantage of the twice larger, 50 mrad, JLEIC crossing angle.

Figure 8 shows how the envelope of the eRHIC IR elements fits into the existing RHIC accelerator tunnel. There is enough space for Crab Cavity cryostats and spin rotator modules (for polarization control) as well as the ZDC and Roman Pots. On the rear side of the eRHIC layout an electron bending dipole deflects the circulating electron beam away from the line of sight from the IP to provide locations for a luminosity monitor and extra bending for a rear scattered electron tagger.

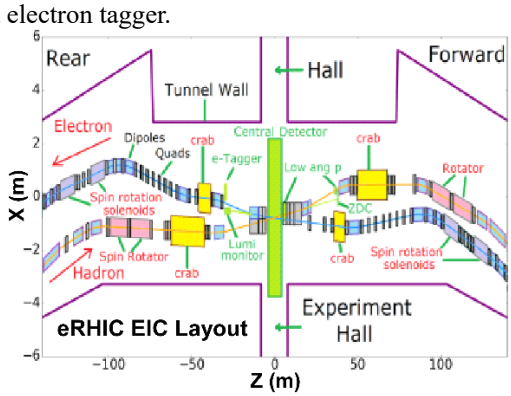


Figure 8: Plot of eRHIC IR accelerator component transverse envelopes, within existing experimental hall and RHIC tunnel, at greatly compressed horizontal scale.

The JLEIC layout uses a four-magnet chicane in place of the eRHIC simple dogleg, that then provides usable space for precision electron polarimetry. The eRHIC precision electron polarimeter is located elsewhere in the same RHIC straight section as the present hadron polarimeters. Both designs provide for a precision luminosity monitor that uses Bethe-Heitler bremsstrahlung photons to count $e^+e^-$ pairs created in a thin conversion target while having an in-line photon calorimeter that is used to give a fast luminosity tuning signal for the accelerator.

The superconducting magnets closest to the central detector have very tight coil spacing between each beam line. An example of this is Fig. 9 which shows a forward side, eRHIC, dual aperture magnet. After considering the required beam apertures, there is just barely space for side-by-side NbTi superconducting coils at each beam. Since the electron quadrupole coil field is much less than that of the larger, high-gradient hadron coil, the main challenge is to provide enough yoke material between the two apertures in order that the hadron field does not appreciably leak into the electron aperture.

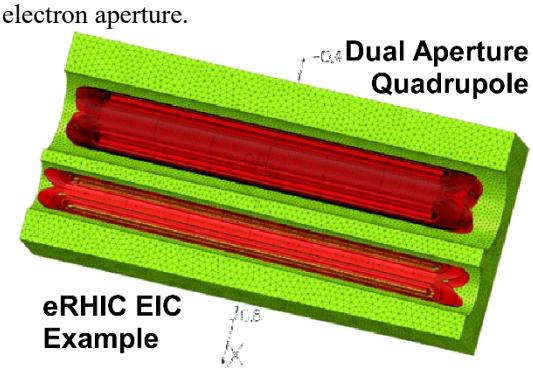


Figure 9: Dual aperture quadrupole magnet with side-by-side NbTi coils in a common magnetic yoke structure.

The rear side situation is quite different; while the electron gradients are still quite modest, their apertures are deliberately increased, in order to pass the synchrotron radiation from the upstream forward side electron quadrupoles completely through the rear side magnets. The solution eRHIC uses to maintain adequate yoke material between the side-by-side coils is to taper the magnet coils and thereby provide extra yoke thickness at the tightest near-IP end of the magnet. In order to simplify beam optics matching, we require the gradient to be constant despite the changing coil radius along the magnet length.

Our prefered method to maintain a constant gradient in a tapered coil is to take advantage of the design flexability inherent with the double helical winding scheme (sometimes known as Canted Cosine Theta) [17]. An example of such a double helical winding is shown in Fig. 10. Double helical coils are wound in pairs as modulated “solenoid like” coils that wrap in opposite directions around the main aperture. The solenoid field from each layer is opposite and cancels, but with opposite conductor pitches in each layer, the transverse field components for each layer add constructively. Since the local transverse field strength depends on the back and forth pitching of the conductor during winding, by smoothly varying the pitch along the coil’s

ISBN: 978-3-95450-223-3 ISSN: 2673-7000 doi:10.18429/JACoW-NAPAC2019-TUZBA2

length we look to offset the natural change in gradient due to change in coil radius.

The R&D coil shown in Fig. 10 was wound using the same Direct Wind technology successfully used for the SuperKEKB IR external field cancel coils [18, 19]. The SuperKEKB cancel coils used short Serpentine winding patterns and the local cancel coil field strength was tuned by stretching out the end turn spacing; however, for very long EIC coils, having widely spaced end turns leads to obvious jumps in local field strength. Since in a double helical pattern the winding pitch can smoothly change, we anticipate it can give a more uniform quadrupole gradient.

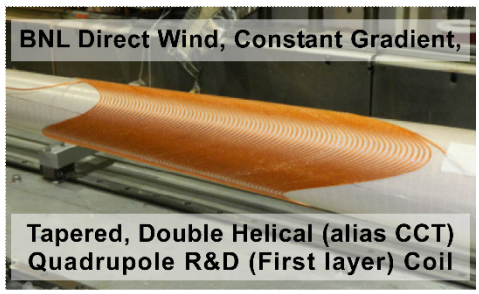


Figure 10: First layer, BNL Direct Wind tapered, double helical, constant gradient quadrupole R&D coil. A second oppositely wound layer cancels the solenoid component but reverses the conductor pitch, so quadrupole remains.

A more traditional Rutherford cable based, cosine theta coil example is the JLEIC IR quadrupole shown in Fig. 11 [20-22]. A challenge addressed with this JLEIC design is to find space for skew-multipole windings needed to address detector solenoid field optical effects (no useful place available for anti-solenoids). The design in Fig. 11 does not rob longitudinal space for these correctors and avoids shortening main magnets. But the outer coil takes up radial space; the design task is to have enough yoke thickness to limit yoke saturation and avoid having unacceptable external fields at the circulating electron beam.

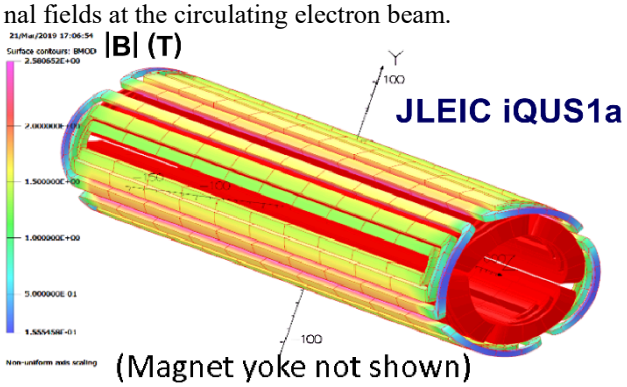


Figure 11: JLEIC quadrupole with added skew winding.

The bare magnet designs discussed so far must be dressed in helium containment vessels and cryostats and then integrated with bellows for warm-to-cold transitions, synchrotron radiation masks and collimators; BPMs, vacuum valves and other technical components. The CAD views in Fig. 12 show an early attempt to capture some of these technical components relative to the experimental detector solenoid.

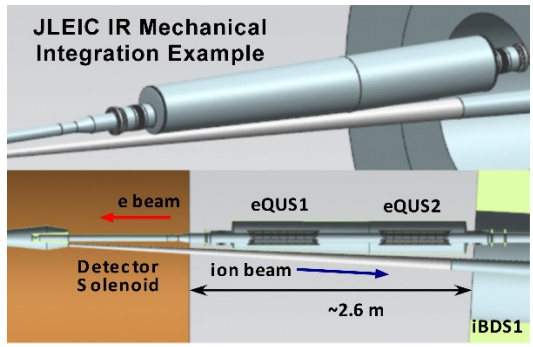


Figure 12: CAD examples of EIC MDI component mechanical integration showing coils, cryostats, bellows etc.

Clearly space in the IR, one of the most complex, crowded regions of the entire accelerator complex, is precious and deserves special attention when interfacing different technical systems and sorting out competing EIC MDI issues. Some of the electron quadrupoles closest to the IR have gradients "weak enough" that they could use warm normal-conducting coils, but they are superconducting because they contact the cold magnetic yokes of the hadron beam line magnets.

Seemingly innocent design choices can impact local beam vacuum levels which in turn have strong implications for detector background. Because the EIC electron circulating beam current and bunch length is comparable to state-of-the-art B-factories, the IR design must address many of the same challenges, namely resistive wall heating, trapped modes, local beam loss and synchrotron radiation heating, while keeping in mind that it is undesirable to increase the cryogenic heat load in a superconducting IR magnet.

The detector beam pipe (a JLEIC detector beam pipe example is shown in Fig. 13), presents a quite singular MDI optimization challenge. The experiment needs to minimize the central pipe wall thickness and outer radius, but the inner aperture should not be reduced so much that it starts intercepting synchrotron radiation. The pipe radius must grow to match separate beam pipes, but any abrupt transitions to the external pipes can lead to trapped modes, excessive beam pipe heating and poor vacuum. An absorptive coating inside the beam pipe could improve the vacuum, but a high resistivity coating could then lead to increased chamber wall heating. Possible mitigations to these challenges, including using smooth tapered wall transitions, local HOM dampers and image current screening are now under intensive study.

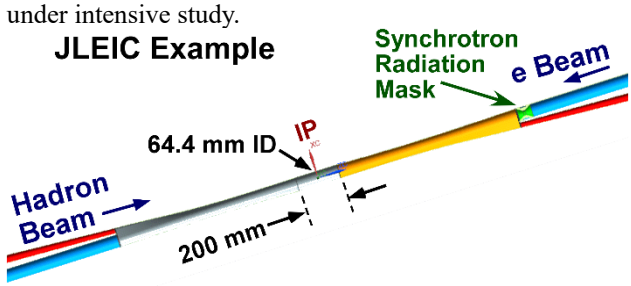


Figure 13: JLEIC detector beam pipe detail.

ISBN: 978-3-95450-223-3 ISSN: 2673-7000 doi:10.18429/JACoW-NAPAC2019-TUZBA2



## ACKNOWLEDGMENT

The work described in this paper and a greater body of work not covered, was performed collaboratively by people in the EIC IR working groups and EIC User Group teams. While they are too numerous to individually credit, the authors of this paper wish to thank everyone for their dedication to our common vision of realizing an EIC as the next high priority US Nuclear Physics project.

## REFERENCES

[1] R. Tribble *et al.*, "The Frontiers of Nuclear Science: A Long Range Plan," DOE/NSF Nuclear Science Advisory Committee, December 2007.

[2] A. Aprahamian *et al.*, "Reaching for the Horizon: The 2015 Long Range Plan for Nuclear Science, October 2015.

[3] A. Accardi *et al.*, "Electron Ion Collider: The Next QCD Frontier - Understanding the Glue that Binds Us All," Eur. Phys. J. A52, p. 268 (2016), DOI: 10.1140/epja/i2016-16268-9.

[4] National Academies of Sciences, Engineering, and Medicine. 2018. "An Assessment of U.S.-Based Electron-Ion Collider Science," Washington, DC: The National Academies Press. DOI: 10.17226/25171.

[5] A. Seryi *et al.*, "The US Electron Ion Collider Accelerator Designs," presented at the North American Particle Accelerator Conference (NAPAC2019), Lansing, MI, USA, September 2019, paper MOOHC2, this conference.

[6] C. Montag *et al.*, "eRHIC Design Update," presented at the North American Particle Accelerator Conference (NAPAC2019), Lansing, MI, USA, September 2019, paper MOYBA4, this conference.

[7] Y. Zhang *et al.*, "JLEIC Design Update," presented at the North American Particle Accelerator Conference (NAPAC2019), Lansing, MI, USA, September 2019, paper MOYBA3, this conference.

[8] B. Parker, R. B. Palmer, and H. Witte, "The eRHIC Interaction Region Magnets", in *Proc. 8th Int. Particle Accelerator Conf. (IPAC'17)*, Copenhagen, Denmark, May 2017, pp. 3624-3626. doi:10.18429/JACoW-IPAC2017-WEPVA151

[9] V. S. Morozov *et al.*, "Full Acceptance Interaction Region Design of JLEIC", in *Proc. 10th Int. Particle Accelerator Conf. (IPAC'19)*, Melbourne, Australia, May 2019, pp. 2787-2790. doi:10.18429/JACoW-IPAC2019-WEPGW123

[10] LHeC Study Group, "A Large Hadron Electron Collider at CERN: Report on the Physics and Design Concepts for Machine and Detector," *J. Phys. G: Nucl. Part. Phys.*, vol. 39, 075001, 2012. doi: 10.1088/0954-3899/39/7/075001

[11] E.C. Aschenauer, A. Kiselev, B. Parker, and R. Petti, "Issues of Incompatibility of Dipole Beam Separation Schemes with EIC Physics," EIC IR Group Design Report, BNL, Nov. 9, 2015, https://erhic.docdb.bnl.gov/cgi-bin/public/ShowDocument?docid=6.

[12] H. Witte, R. B. Palmer, and B. Parker, "Options for the Spectrometer Magnet of the eRHIC IR", in *Proc. 9th Int. Particle Accelerator Conf. (IPAC'18)*, Vancouver, Canada, Apr.-May 2018, pp. 2401-2403. doi:10.18429/JACoW-IPAC2018-WEPMF017

[13] B. Parker *et al.*, "Fast Track Actively Shielded Nb3Sn IR Quadrupole R&D", in *Proc. 9th Int. Particle Accelerator Conf. (IPAC'18)*, Vancouver, Canada, Apr.-May 2018, pp. 2398-2400. doi:10.18429/JACoW-IPAC2018-WEPMF014

[14] R. Rajput-Ghoshal, *et al.*, "Conceptual Design of the Interaction Region Magnets for Future Electron-Ion Collider at Jefferson Lab", *IEEE Trans. Appl. Supercond.*, vol. 29, issue: 5, August 2019. doi: 10.1109/TASC.2019.2901590

[15] M. Wiseman *et al.*, "Preliminary Design of the Interaction Region Beam Transport Systems for JLEIC," *Appl. Supercond.*, vol. 29, issue: 5, August 2019. doi:10.1109/TASC.2019.2896378

[16] B. Parker, R. B. Palmer, and H. Witte, "An Improved eRHIC Interaction Region Design Without High Field $Nb_3Sn$ Magnets", in *Proc. 10th Int. Particle Accelerator Conf. (IPAC'19)*, Melbourne, Australia, May 2019, pp. 799-801. doi:10.18429/JACoW-IPAC2019-MOPRB100

[17] H. Witte, B. Parker, and R. Palmer, "Design of a Tapered Final Focusing Magnet for eRHIC," *IEEE Trans. Appl. Supercond.*, vol. 29, issue 5, pp. 1-5, Aug. 2019. doi: 10.1109/TASC.2019.2902982

[18] B. Parker *et al.*, "Superconducting Corrector IR Magnet Production for SuperKEKB", in *Proc. North American Particle Accelerator Conf. (NAPAC'13)*, Pasadena, CA, USA, Sep.-Oct. 2013, paper THPBA07, pp. 1241-1243.

[19] B. Parker, *et al.*, "BNL Direct Wind Superconducting Magnets," *IEEE Trans. Appl. Supercond.*, vol. 22, issue 3, 2012. doi: 10.1109/TASC.2011.2175693.

[20] R. Rajput-Ghoshal, *et al.*, "Interaction Region Magnets for Future Electron-Ion Collider at Jefferson Lab", presented at the North American Particle Accelerator Conference (NAPAC2019), Lansing, MI, USA, September 2019, paper TUZBA4, this conference.

[21] M. Anerella, *et al.*, "Design of a Compact Support Structure for a High Gradient Niobium Tin Superconducting Magnet for a Proposed Electron Ion Collider (EIC)," presented at the MT26 International Conference on Magnet Technology, Vancouver, Canada September 2019.

[22] R. Rajput-Ghoshal, *et al.*, "Optimization of an Interaction Region Quadrupole Magnet for Future Electron-Ion Collider at Jefferson Lab," presented at the MT26 International Conference on Magnet Technology, Vancouver, Canada September 2019.